

Article

Stabilization Study of a Contaminated Soil with Metal(loid)s Adding Different Low-Grade MgO Degrees

Jessica Giro-Paloma , Joan Formosa  and Josep M Chimenos 

Departament de Ciència de Materials i Química Física, Universitat de Barcelona, 08028 Barcelona, Spain; joanformosa@ub.edu (J.F.); chimenos@ub.edu (J.M.C.)

* Correspondence: jessicagiro@ub.edu; Tel.: +34-93403-72-44

Received: 31 July 2020; Accepted: 3 September 2020; Published: 7 September 2020



Abstract: Low-grade magnesium oxide (LG-MgO) was proposed as ordinary Portland cement (OPC) or lime substitute (CaO) for metal(loid)s remediation in contaminated soils. Some metal(loid)s precipitate at $\text{pH} \approx 9$ in insoluble hydroxide form thus avoiding their leaching. LG-MgO avoids the re-dissolution of certain metal(loid)s at $9.0 < \text{pH} < 11.0$ (pH-dependents), whose solubility depends on the pH. A highly contaminated soil with heavy metal(loid)s was stabilized using different LG-MgO by-products sources as stabilizing agents. Two of the three studied LG-MgOs were selected for the stabilization, by mixing 5, 10, and 15 wt.%. The effect of using LG-MgO not only depends on the size of the particles, but also on those impurities that are present in the LG-MgO samples. Particle size distribution, X-ray fluorescence (XRF), X-ray diffraction (XRD), thermogravimetric analysis, citric acid test, specific surface, bulk density, acid neutralization capacity, batch leaching tests (BLTs), and percolation column tests (PCTs) were techniques used to deeply characterize the different LG-MgO and the contaminated and remediated soils. The remediation's results efficacy indicated that when the medium pH was between 9.0 and 11.0, the concentration of pH-dependent metal(loid)s decreases significantly. Although around 15 wt.% of a stabilizing agent was appropriate for the soil remediation to ensure an alkali reservoir that maintains optimal stabilization conditions for a long period, 5 wt.% of LG-MgO was enough to remedy the contaminated soil. When evaluating a polluted and decontaminated soil, both BLTs and PCTs should be complementary procedures.

Keywords: polluted soil; LG-MgO; soil stabilization; magnesium oxide by-products; percolation column test; batch leaching test; waste valorization

1. Introduction

The incidence and availability of heavy metals and metalloids in soils is the main issue affecting environmental health, crop and livestock production, food and water quality, and eco-toxicology [1]. The concentrations of metal(loid)s in soils can differ extensively in non-contaminated and contaminated soils. Concerning contaminated soils, the contamination of metal(loid)s can produce toxicity, although it would depend on the factors which affect the bioavailability of the elements. According to their solubility, the leaching of heavy metals and metalloids to natural currents of groundwater, rivers, and the sea is an important environmental issue. There are several mechanisms that allow metal(loid)s to move around and leave a soil such as leaching, which occurs when the water seeps through the soil. The pH of natural rainfall is between 5.5 and 5.6 due to its interaction with CO_2 present in the atmosphere [2]. Depending on the type of the soil and its characteristics, the leaching of metal(loid)s can be considerable [3]. The two ways for remediation of metal(loid)-contaminated soils are the oxidation states modification of the metal(loid)s (changing their chemical composition) and

the elimination or extraction of the metal(loid)s from the soils [4]. Therefore, the mobilizing and the immobilizing techniques are the two categories for the metal(loid)s' remediation contained in contaminated soils [5]. While the former focuses on the intensive extraction of metal(loid)s in processing plants, the immobilizing techniques stabilize heavy metal(loid)s through adsorption, complexation, or precipitation reactions, avoiding the leaching phenomenon [6]. The immobilizing techniques are usually cheaper than the mobilizing ones, which are often very expensive in terms of energy and economy [7]. One of the immobilization conditions is referred to as the monitorization of the immobilized heavy metal(loid)s' long-term stability [7,8]. The immobilization mechanisms include precipitation, chemical adsorption and ion exchange, surface precipitation, the formation of stable complexes with organic ligands, and redox reaction [9]. Immobilization technologies can be performed *ex situ* or *in situ*. Although *in-situ* processes depend on specific site conditions, they are preferred because of the lower energy requirements.

Several authors have investigated the remediation of Cu, Zn [10], Cd, and Pb [11–17] in environmental samples, all of them referred to as pH-dependent metals. Furthermore, the most cost-effective and capable option for contaminated soils with metal(loid)s is the stabilization/solidification treatment processes by means of adding chemical additives to the soil [18]. In this kind of remediation process, the neo-formed compounds cannot be dissolved easily in water, neither spread in water media to pollute streams or other groundwater. On the other hand, it is known that in an alkaline medium the Pb and other pH-dependent metal(loid)s generate their corresponding hydroxides, which show their minimum solubility within the pH range of 9–11 [19–22] and, consequently, their mobility decreases. Below and above this pH range, these pH-dependent metal(loid)s are re-dissolved and can be released into aqueous media.

It is well-known that the application of ordinary Portland cement (OPC) or lime (CaO) increase the soil pH and decrease metal availability [23,24]. Nevertheless, in accordance with its solubility reaction equilibrium, magnesium (hydr)oxide is a proper chemical stabilizer, as it acts as a buffering agent in the 9–11 pH range. However, due to the high cost of high pure MgO/Mg(OH)₂, a possible alternative to stabilize pH-dependent metal(loid)s from contaminated soils is the usage of MgO by-products or low-grade MgO (LG-MgO), according to previous studies [22]. Adding the proper amount of LG-MgO obtains the optimal pH range, like in the case of pure magnesium (hydr)oxide, and an extra addition does not affect the pH value of the remediated soil, offering an alkali reservoir, assuring long-term stabilization without changing the pH conditions [1]. Accordingly, the addition of LG-MgO allows the *in-situ* remediation by means of the stabilization of pH-dependent metal(loid)s and it does not disrupt the environment or generate hazardous wastes. It is reported elsewhere [22] that the use of LG-MgO as an alkali stabilizer for the treatment of contaminated soils by metal(loid)s guarantees important rates of reduction of metal(loid)s, greater than 80 wt. %. Likewise, the addition of by-products or LG-MgO as a stabilizing source in the remediation of soils addresses two issues: (1) it becomes possible to reuse a by-product that follows the path towards sustainability, contributing to the principles of the circular economy, and (2) an environmental solution is attained by means of an environmentally friendly agent.

Against the above background, the effectiveness of LG-MgO as a stabilizing agent in contaminated soils containing pH-dependent metal(loid)s can be established based on its reactivity and its behavior across the whole pH range [25]. Both chemical properties are directly related to their specific surface area and particle size distribution [26]. While the reactivity of magnesium (hydr)oxide is usually determined using the citric acid test (CAT), measuring the time needed to neutralize this weak acid [27], the acid neutralization capacity (ANC) test [28] allows measuring the buffering capacity and determines the ability to maintain a stable pH range.

The goal of this study aims to evaluate the potential use of different LG-MgO by-product sources to be used as alkali stabilizers of heavy metals and metalloids in contaminated soil. For this purpose, their chemical and mineralogical composition as well as various physical properties were evaluated. Likewise, the ANC test was used as a tool to predict their effectiveness as stabilizing agents for remediation and their buffering capacity. Moreover, the remediation of polluted industrial

soil by adding different proportions of different LG-MgO sources, as stabilizing agents, to obtain a remediated soil was evaluated. When evaluating both polluted and decontaminated soils, the dynamic leaching tests batch leaching test (BLT) (EN-12457-4) and percolation column test (PCT) [29,30] are complementary procedures to study. Hence, the effectiveness of the different LG-MgO by-products sources used as stabilizers mixed with the contaminated soil must be studied, evaluated, and compared.

2. Materials and Methods

2.1. Materials

2.1.1. Contaminated Soil

The contaminated soil (CONSO) sample was collected in the brownfield lands of an old company, about 40 km west of Barcelona (Spain), and engaged to the recycling of cathodes and anodes of the lead–acid batteries. During the recycling metallurgical processes, the wastes were indiscriminately disposed of in the surrounding lands, which included slag from lead and/or fine filtering powder. Because of the long-term deposition of wastes, these were exposed to atmospheric conditionings (e.g., rainfall) and the dissolved metal(loid)s were released, significantly affecting the soil over which they were discharged. The soil on which the wastes were deposited was formed by heteromeric clean sands and gravels, mainly constituted by silica matrix, i.e., feldspars and quartz, with the scant presence of slimes. Most of the CONSO area was fully covered by a variable thickness of the deposited roasting pyrite and other wastes generated during the metallurgical process.

2.1.2. Low-Grade Magnesium Oxides

Three types of low-grade magnesium oxides (LG-MgOs) were considered in this study, differing mainly in their particle size and Mg/Ca content. Samples of the three types of LG-MgO were supplied by Magnesitas Navarras S.A., located in Navarra (Spain). All the LG-MgO sources were generated during the calcination of natural magnesite in rotary kilns. The first source of LG-MgO under consideration corresponded to the fly particles collected in the fabric filters of the pollution control system of the exhaust gases generated when obtaining hard-burned caustic magnesia and sintered magnesia, at 1200 °C and 1600 °C, respectively. The dust material collected is named PC8 and it is classified as a by-product of the combustion process. The second LG-MgO considered, called MCB100, is caustic magnesia obtained during the calcination of natural magnesite in a rotary kiln at a temperature around 750–800 °C. At this temperature range, only magnesite (MgCO_3) is thermally decarbonized, while dolomite ($\text{MgCa}(\text{CO}_3)_2$) and calcite (CaCO_3) remain unchanged. The third LG-MgO under study, MCB100M, is the product obtained after a grinding process of the MCB100. Both caustic magnesia (MCB100 and MCB100M) have the same bulk composition, although they show a great difference in the particle size. With these three types of LG-MgO, the magnesium content effect, the reactivity and the ANC of LG-MgO, and the buffered pH of the remediated soil (REMSO) were studied.

Around 25 kg of each LG-MgO under study were taken from various stockpiles. Afterward, the CONSO stabilization was evaluated by adding different percentages of the three different LG-MgOs: 0, 5, 10, and 15 wt.% in dry content.

2.2. Methods

The standard EN 932-1 was followed as a method for sampling and to select a representative sample of 2 kg of CONSO, which was quartered with a splitter. Afterward, it was sieved until it had a particle size below 10 mm.

BLTs were performed to the CONSO to evaluate the metal(loid)s release, following the standard EN 12457-4. It consists of placing a solid in contact with deionized water in a liquid-solid (L/S) ratio of 10 L/kg during 24 h with continuous rotating agitation. An OVAN orbital shaker was used to perform the tests in high-density polyethylene (HDPE) containers. The acid neutralization capacity (ANC) test

was also conducted according to standard [28] and following previous studies [25] by adding nitric acid, with a concentration of 65% from labKem company. The sample was subjected to consecutive and ordered acid additions, in order to obtain a curve of pH vs. hydronium (H_3O^+) per mass of solid. Different volumes of HNO_3 (65 wt.%) were added to gradually decrease pH to 4.0.

The different LG-MgO stabilizing agents under study (PC8, MCB100, and MCB100M) were characterized in order to explain their different characteristics and properties. Particle size distribution (PSD), X-ray fluorescence (XRF), X-ray diffraction (XRD), thermogravimetric analysis (TGA), citric acid test (CAT), specific surface (BET), bulk density, and ANC techniques were used to characterize the LG-MgO. A Beckman Coulter LS 13.320 device with the universal liquid module was used to evaluate the PSD in volume percentage of the three different LG-MgOs under study. To study the most stable oxides, XRF was used by means of a Panalytical Philips PW2400 X-ray sequential equipped with the software UniQuant[®] V5.0 spectrophotometer. XRD was performed to evaluate their crystallographic phases using a Bragg–Brentano Siemens D-500 powder diffractometer with $\text{CuK}\alpha$ radiation and processing the data by the X'Pert Highscore software. Manual pressing was used by means of a glass plate to get a flat surface, in cylindrical standard sample holders of 16 mm of diameter and 2.5 mm of height. The chemical constitution determination was conducted by means of TGA, and the procedure consisted of a heating rate of $10\text{ }^\circ\text{C}\cdot\text{min}^{-1}$ from $30\text{ }^\circ\text{C}$ to $1200\text{ }^\circ\text{C}$ in N_2 atmosphere ($50\text{ mL}\cdot\text{min}^{-1}$). In parallel, CATs were performed to the three different LG-MgOs to elucidate the reactivity of the LG-MgO samples until $\text{pH} = 9.0$ [25]. The CAT was done by reaching a neutralization reaction between the citric acid and the basic oxides of the LG-MgO samples such as MgO or CaO, where the time required to reach a certain pH was evaluated. Acid neutralization values of less than 60 s were used to define highly reactive (soft burnt) MgO. Medium reactive MgO gives a measure between 180 and 300 s, while a low reactivity MgO (hard-burnt) and a dead-burnt MgO give values greater than 600 s and 900 s respectively [27]. Specific surface area BET single point method was performed with a Micrometrics Tristar 3000 porosimeter. For the bulk density, a helium pycnometer was used. The last test performed to the different LG-MgO by-products under study was the ANC test to select the minimum percentage of LG-MgO required to reach the optimal pH for minimal metal(loid) release [22].

After studying both the CONSO and the different LG-MgO stabilizing agents, different formulations were prepared, adding and mixing to the contaminated soil 0, 5, 10, and 15 wt.% of LG-MgO to obtain REMSO samples. The ANC test, the BLT, and the PCT were performed on the different REMSO samples. Regarding the ANC assay, it allows discerning the buffering capacity of the REMSO; that is, the acid resistance offered by REMSO depends on the different percentage of LG-MgO added to CONSO. At a higher buffering capacity, the pH is more stable over a long range of acid additions [25]. Concerning the BLT, the same procedure was followed as for the CONSO samples, where two replicates were tested for each formulation. Finally, the PCT was performed on the REMSO following the standard CEN/TS 16637-3 [29]. If all the distilled water is considered to pass through the percolation column, an extrapolation of the time to real years can be performed (durability evaluation), considering the following parameters: (i) surface, (ii) thickness, (iii) average rainfall, (iv) percolation column volume, and (v) relation of $10\text{ L}\cdot\text{kg}^{-1}$. The PCTs consisted of placing 1 kg of dry soil with 5, 10, and 15 wt.% of LG-MgO in a cylindrical column and flooding it with deionized water. Then, the deionized water passed through from the bottom of the column to the top (bottom-up) with the help of a pump, set at $24\text{ mL}\cdot\text{h}^{-1}$. Therefore, the ability of the different LG-MgO samples to give a pH in the range of minimum solubility of metal(loid)s after three weeks were studied.

For both dynamic leaching trials performed, the BLT and the PCT, the leachates obtained were filtered through a $0.45\text{ }\mu\text{m}$ membrane of nitrocellulose, and two aliquots of each leaching condition were collected for further analysis by means of inductively coupled plasma mass spectrometry (ICP-MS). Likewise, pH, conductivity (k), and Cr^{6+} of the leachates were also analyzed in order to compare the behavior of CONSO and REMSO. A Crison GLP 22 pH meter, a Crison EC-Meter 30+ conductivity meter, and an Aquamater Thermosprectronic spectrophotometer with a reagent kit to determine Cr^{6+} were used.

3. Results and Discussion

3.1. Contaminated Soil Characterization

The mean value results of CONSO BLTs following the EN 12457-4 standard are shown in Table 1, where the values are determined per duplicate. The release of metal(loid)s was relevant, denoting hazardous values for As and Pb and non-hazardous values for Cd and Sb species. It is important to highlight that the rest of the elements remained below the inert limits.

Table 1. Results of leaching concentration values in $\text{mg}\cdot\text{kg}^{-1}$ for the contaminated soil (CONSO) classified depending on the landfill threshold values. CONSO pH = 6.95 and $k = 2.49 \text{ mS}\cdot\text{cm}^{-1}$.

Metal(loid)s ($\text{mg}\cdot\text{kg}^{-1}$)	CONSO	Landfill Thresholds		
		Inert	Non-Hazardous	Hazardous
As	3.12	0.5	2	25
Ba	0.14	20	100	300
Bi	0.01	-	-	-
Cd	2.78	0.04	1	5
Co	<0.03	-	-	-
total Cr	<0.10	0.5	10	70
Cr ⁶⁺	<0.20	-	-	-
Cu	0.36	2	50	100
Hg	<0.01	0.01	0.2	2
Mo	<0.01	0.5	10	30
Ni	0.28	0.4	10	40
Pb	137.7	0.5	10	50
Sb	2.10	0.06	0.7	5
Sn	0.05	-	-	-
V	<0.05	-	-	-
Zn	2.37	4	50	200

According to the results obtained for the ANC test, the pH decreases with small acid quantities, which reveals a lack of buffering capacity in CONSO, as Figure 1 shows. The natural pH of the polluted soil started at pH around 7.0 and after adding a very little amount of HNO_3 1M the pH dropped down. Then, the remediation of CONSO using LG-MgO as an alkaline stabilizing agent was evident due to (i) the natural pH obtained (6.95), (ii) the low buffering capacity showed in Figure 1, and (iii) the release of metal(loid)s shown in Table 1.

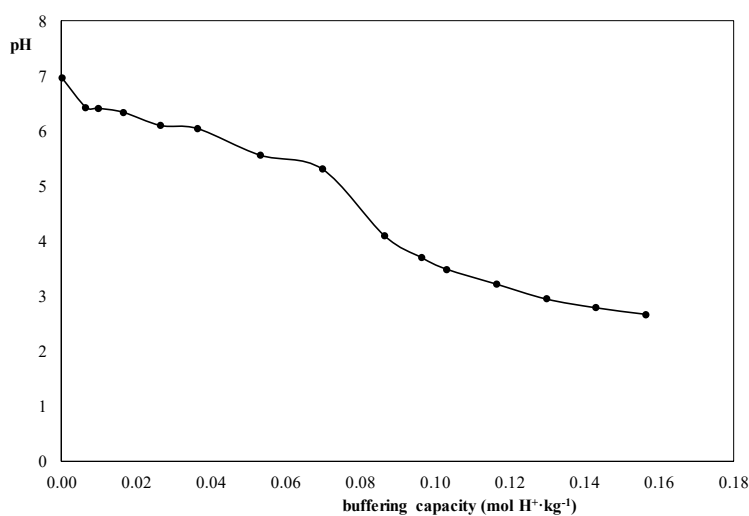


Figure 1. Acid neutralization capacity (ANC) test results for the CONSO.

3.2. LG-MgO Characterization

The PSD in volume percentage for each LG-MgO sample under study is presented in Table 2. Accordingly, the sample which presented the coarse size was MCB100. Meanwhile, PC8 and MCB100M samples presented similar values (same magnitude) for most of the percentages.

Table 2. Particle size in volume percentage of the different low-grade magnesium oxides (LG-MgOs) under study.

LG-MgO	μm				
	d_{10}	d_{25}	d_{50}	d_{75}	d_{90}
PC8	1.68	6.99	21.09	41.55	87.57
MCB100	102.10	168.00	279.80	445.60	764.70
MCB100M	1.18	5.41	14.42	28.09	103.20

Notes: d_x : corresponding to the percentages 10%, 25%, 50%, 75%, and 90% of particles under the reported particle size (μm).

XRF results for the different LG-MgOs under study are shown in Table 3. The samples with a higher content of MgO were MCB100 and MCB100M; meanwhile, PC8 presented higher values of CaO, SO_3 , and loss on ignition (LOI) than MCB100 and MCB100M because this by-product was obtained as cyclone dust in the rotary kiln, and there are mineral phases that do not decompose during the calcination process, among the acid gases from the decomposition that react with alkaline particles, which explains the higher content of SO_3 determined by XRF [31]. It can be detected that all the samples under study contained a small percentage of Al and Fe and about 3 wt.% of SiO_2 .

Table 3. X-ray fluorescence (XRF) results from the three LG-MgO samples.

Oxides (%)	PC8	MCB100	MCB100M
MgO	61.72	83.63	84.31
CaO	9.32	3.25	3.03
SiO_2	2.70	3.04	2.72
Fe_2O_3	2.43	2.94	2.88
Al_2O_3	0.55	0.71	0.62
SO_3	6.55	0.29	0.17
LOI	Loss on Ignition (1050 °C)		
	16.73	6.14	6.27

XRD analysis was conducted for each LG-MgO sample. As expected, magnesium was present mainly as periclase (MgO) in all LG-MgO samples used as stabilizing agents. In addition to periclase, dolomite ($\text{CaMg}(\text{CO}_3)_2$), quartz (SiO_2), anhydrite (CaSO_4), brucite ($\text{Mg}(\text{OH})_2$), calcite (CaCO_3), and magnesite (MgCO_3) were also determined as main mineralogical phases in the PC8 sample. Regarding MCB100 and MCB100M (both have the same nature), in addition to periclase, magnesite (MgCO_3), quartz (SiO_2), brucite ($\text{Mg}(\text{OH})_2$), dolomite ($\text{MgCa}(\text{CO}_3)_2$), calcite (CaCO_3), and anhydrite (CaSO_4) were also determined as main mineralogical phases.

MCB100 and PC8 samples were analyzed by TGA to estimate the percentage of the aforementioned mineralogical phases. Moreover, TGA results were compared with those XRF results. The TGA experiment results and the corresponding derivative weight are shown in Figure 2, where blue and black lines are referred to as PC8 and MCB100 in the manuscript online version, respectively.

The weight loss percentage for each decomposition (Figure 2a) and the temperature in the maximum rate of decomposition (Figure 2b) can be observed to clarify the assignment of each mass loss step. These decomposition steps can be ascribed to the moisture (below 105 °C) and the water of crystallization loss (below 200 °C; attributed to the formation of $\text{CaSO}_4 \cdot 2\text{H}_2\text{O}$), $\text{Mg}(\text{OH})_2$ decomposition

to MgO (from ≈ 250 °C to ≈ 450 °C), MgCO_3 decomposition to MgO and CO_2 (between ≈ 450 °C and ≈ 625 °C), $\text{CaMg}(\text{CO}_3)_2$ decomposition to MgO (between ≈ 625 °C and ≈ 750 °C), and CaCO_3 decomposition to CaO and CO_2 (between ≈ 760 and ≈ 1000 °C). The decomposition of CaSO_4 between 1100 and 1200 °C was also observed.

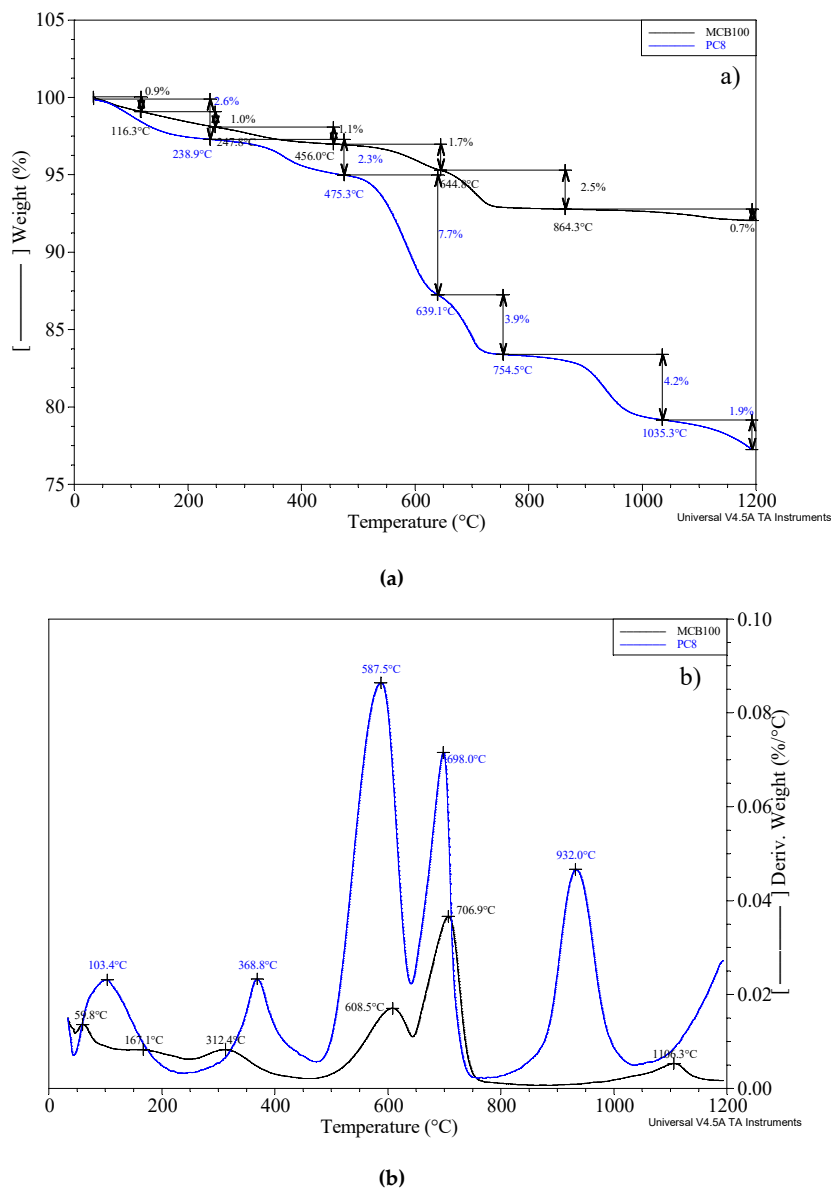


Figure 2. (a) Thermogravimetric analysis (TGA) experiment in N_2 atmosphere and (b) the corresponding derivative of weight of MCB100 (black line in online version) and PC8 (blue line in online version).

Considering the XRD and TGA decomposition results, the range temperature, and stoichiometry, the percentage of each compound was determined. Table 4 presents the compound assignment of each decomposition according to the temperature at the maximum decomposition rate (T_{max}) as well as the weight loss percentage during the TGA test of each sample. The compounds' weight percentages were calculated by considering, in each case, the decomposition reaction stoichiometry [31] and the weight percentage of decomposition for each case (i.e., from Figure 2 and Table 4). Comparing the results obtained in Tables 3 and 4, an estimation of MgO and CaO content in the samples was conducted (for instance in the case of PC8: 8.2 wt.% of $\text{CaMg}(\text{CO}_3)_2$ implies a 1.8 wt.% of MgO in XRF, 2.5 wt.% of CaO in XRF, and 3.9 wt.% of CO_2 or LOI in XRF). Therefore, Table 5 summarizes the most relevant compounds in the samples under study. From the knowledge of the authors and considering the XRD

phases detected, it would be concluded that the MgO amount was around 50% for PC8 and 80% in the case of MCB100 and MCB100M.

Table 4. Compound assigned by means of the temperature at the maximum rate of decomposition and weight percentage loss.

Compound	MCB100		PC8	
	T _{max} (°C)	Weight Loss (%)	T _{max} (°C)	Weight Loss (%)
Humidity (H ₂ O)	59.8	0.9	103.4	2.6
CaSO ₄ ·2H ₂ O	167.1	1.0	-	-
Mg(OH) ₂	312.4	1.1	368.8	2.3
MgCO ₃	608.5	1.7	587.5	7.7
CaMg(CO ₃) ₂	706.9	2.5	698.0	3.9
CaCO ₃	-	-	932.0	4.2
CaSO ₄	1106.3	0.7	above 1200.0	> 1.9

Table 5. Estimation of MCB100 and PC8 composition.

Compound	Weight (%)	
	MCB100	PC8
MgO	78.5	47.7
MgCO ₃	3.3	14.8
CaCO ₃	0.0	9.6
CaMg(CO ₃) ₂	5.2	8.2
Mg(OH) ₂	3.6	7.5
CaSO ₄	1.2	3.2
H ₂ O (humidity)	0.9	2.6
CaO	1.2	0.2
Others	6.1	6.2

BET and the bulk density results as well as the CAT assay results are in Table 6. According to the required time (s) to reach pH 9.0 (CAT), the reactivity of each LG-MgO was classified as follows: MCB100 is classified as medium reactive MgO, MCB100M as soft-burnt MgO (highly reactive), and PC8 is classified as dead-burnt MgO. The difference in the CAT results between both MCB100 samples should be attributed to the particle size distribution. Moreover, the greater the specific surface, the greater the reactivity.

Table 6. BET, bulk density, and citric acid test (CAT) results for LG-MgO samples.

LG-MgO	BET (m ² ·g ⁻¹)	Bulk Density (g·cm ⁻³)	CAT Time at pH = 9 (s)
PC8	5.25 ± 0.04	2,8621 ± 0.0005	1320
MCB100	14.81 ± 0.08	3,0984 ± 0.0005	460
MCB100M	49.69 ± 0.09	3,2467 ± 0.0003	60

Some of the alkali species contained in the LG-MgO upon contact with water would establish a solubility equilibrium resulting in their corresponding hydroxide. Thus, depending on the type of LG-MgO, the composition of the oxides could vary as well as their mineralogical phases, affecting the ANC curves results. In order to explain these pieces of evidence, three phases of the ANC curves and the equilibrium established in each of the samples are described [25]. The different ANC curves for the three types of LG-MgO under study are shown in Figure 3 and, for all the samples under study, the first phase was considered in a pH range between 12 and 10.5, the second phase was identified by a pH stabilization between 10.5 and 8.5 in a wide range of acid additions, and finally, the third phase was considered from 8.5 < pH < 4.

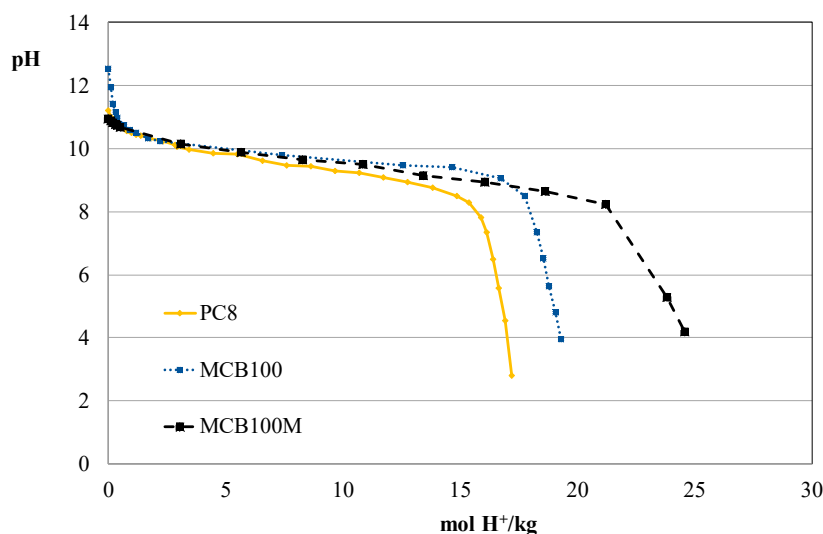


Figure 3. LG-MgO ANC results.

This first phase is controlled by the solubility equilibrium of lime (CaO), close to pH 12.2 and characterized by an abrupt drop in pH caused by an addition of a small amount of nitric acid ($\text{mol H}_3\text{O}^+$), or the solubility equilibrium of brucite ($\text{Mg}(\text{OH})_2$) close to pH 10.5 ($K_{\text{ps Mg}(\text{OH})_2} = 1.8 \cdot 10^{-11}$). Accordingly, while the pH of MCB100 was controlled by the portlandite, the pH of PC8 and MCB100M were controlled by the brucite. The different behavior between the MCB100 and MCB100M samples was attributed to particle size distribution. By decreasing the particle size (i.e., MCB100M), the reactivity increased, and the free lime was completely carbonated quickly. The reaction was displaced towards the control of $\text{Mg}(\text{OH})_2$ in those stabilizing agents where the initial pH was controlled by portlandite (i.e., MCB100). This is because the added HNO_3 consumed the CaO in the first stage. The second phase was controlled exclusively by the solubility equilibrium of $\text{Mg}(\text{OH})_2$, which acts as a buffering agent. The third phase on the ANC results was exclusively controlled by the equilibrium of HCO_3^- and CO_3^{2-} [32]. An abrupt decrease in the pH by adding a small amount of HNO_3 is observed, due to the low weight percentage of carbonated mineral phases (see Table 5). It is important to mention that the Al_2O_3 , SiO_2 , and Fe_2O_3 present in the LG-MgO samples did not affect the remediation of CONSO, and scarcely influence in the ANC curve since these last oxides remained inert and virtually unchanged in their precipitated form during the stabilization process. In the light of these results, MCB100M, MCB100, and PC8 exhibit proper ANC, since it was 18.14, 15.98, and 13.86 $\text{mol H}^+ \cdot \text{kg}^{-1}$, respectively, in order to exceed the range of pH 10.5–8.5. Then, as a conclusion for the ANC assay for the LG-MgO samples, when MgO and specific surface of particles increase, the ANC and buffering capacity per unit mass of the stabilizing agent increase, as well. However, together with a high ANC value, it is also necessary to establish a reservoir of the alkali to guarantee a pH buffering capacity in the optimum range over a long period. In this regard, LG-MgO with very low reactivity (e.g., PC8), would be required to maintain the optimal conditions over time. In addition, it must be considered that PC8 is cheaper than MCB100M. Consequently, PC8 and MCB100M were selected as optimum LG-MgOs to stabilize the contaminated soil, due to the cost and because of the reactivity, respectively. PC8 is five to six times cheaper than MCB100M.

3.3. Remediation of the Contaminated Soil

The ANC comparative results after the remediation of the contaminated soil (REMSO) are shown in Figure 4. As expected, it is observed that the buffering capacity of MCB100M used as the stabilizing agent was higher than PC8, because MCB100M contains a higher percentage of MgO (Table 5) and also showed higher ANC per unit mass of stabilizing agent added (Figure 3), which provide a greater reservoir of alkaline stabilizer. Consequently, in the pH range of minimum solubility of metal(loid)s

(pH \approx 8.5–10.0), MCB100M acquired higher buffering capacity than PC8. Increasing the addition of the stabilizing agent (PC8 or MCB100M) also increases the reservoir of alkali and the neutralizing capacity of the remediated soil.

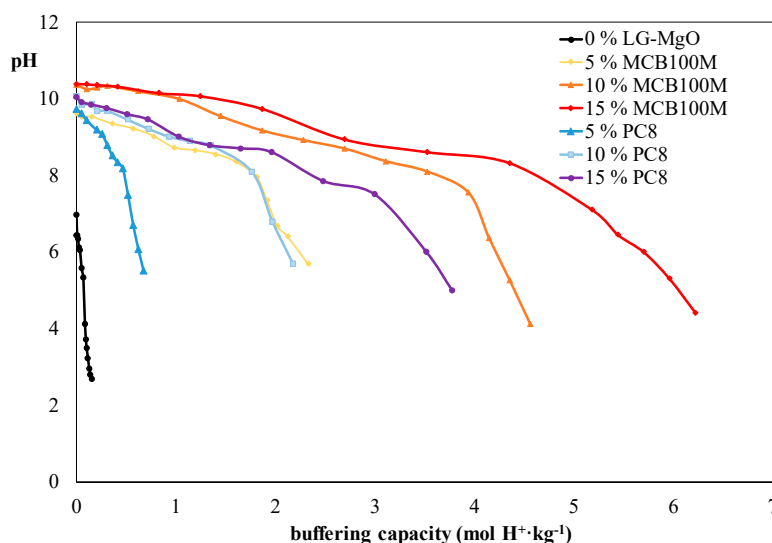


Figure 4. ANC results for the remediated soil (REMSO) with 0, 5, 10, and 15 wt.% of MCB100M and PC8.

It is well-known that both redox potential and pH deeply affect and interfere with the heavy metal solubility in soil. In this case, the pH effect was more significant than that of redox potential. Therefore, this study focused on the pH-dependent evaluation. The pH-dependent metal adsorption reaction and the pH between 9 and 11 were the mechanisms to control the release of heavy metals from the soil. Table 7 shows the REMSO BLT EN 12457-4 mean results, determined per duplicate. It can be denoted that all LG-MgOs achieved the minimum concentration of metal(loid)s, considering the threshold landfill legislation (Table 1). The potential release of As and Sb diminished when the pH of the medium increased, showing a pH-dependent behavior of both metal(loid)s, which mainly denoted the presence of trivalent As and Sb mineral species into CONSO. In these cases, the decrease in pH-dependent metalloids is mainly due to the formation of their corresponding insoluble hydroxides. As(III) and Sb(III) present the minimum solubility forming their corresponding hydroxide when pH is in the alkaline region and high pH (pH < 11 for As(III) and pH < 12 for Sb(III)). As(III) and Sb(III) hydroxides present lower solubility than AsO_4^{3-} , SbO_3^- , and Sb(OH)_6^- , which are soluble. The presence of calcium in the stabilizers helps the formation of calcium arsenates and calcium antimony with low solubility. The same argument justified the leaching decrease for most of the pH-dependent heavy metals. The concentration decrease observed in Cd and Zn was noticeable—greater than 95% in both cases. Surprisingly, the decrease in Pb concentration was lower than expected, compared to previous work [22]. Unexpectedly, the minimum solubility was obtained at pH around 8.5, by adding the minimum amount of either LG-MgO used as a stabilizing agent. By increasing the addition of LG-MgO and increasing the pH of the medium, the total Pb concentration released increased as well. At pH close to 10.5, where minimal solubility would be expected if the Pb concentration was controlled by the solubility of lead hydroxide, the lead released was roughly equal to that of the non-stabilized soil. No significant differences were found when using either of the two LG-MgOs studied. This can be attributed to the content of lead sulfate (anglesite) in the polluted soil. This lead compound is found in large quantities in the spent lead–acid batteries [33]. In this scenario, as indicated by Visual MINTEQ (v. 3.0/3.1) geochemical modeling software version 3.1, the Pb concentration is controlled by the solubility of lead sulfate. In this case, the concentration of the chemical species $\text{Pb(SO}_4)_2^{2-}$ (aq) increases by increasing the pH of the medium.

Even with the high amount of Pb contained in CONSO, both LG-MgOs succeeded in reducing around 70% the leaching content of Pb with 5 wt.% LG-MgO. Then, all values were below the inert or non-hazardous threshold landfill classification, except for Pb where its concentration is above the limits for non-hazardous waste. Thus, according to the BLT EN 12457-4, the optimal percentage for both LG-MgO was 5 wt.%.

Although the behavior of both LG-MgOs was very similar in the BLTs, the column test was tested only with PC8 as a stabilizing agent. The main reason is because of the by-products price, where PC8 is five to six times cheaper than MCB100M. Then, the PCTs (CEN/TS 16637-3) were carried out by using CONSO mixed with 5, 10, and 15 wt.% of PC8, separately. Results per duplicate are shown in Table 8 and, in general, increasing the percentage of PC8 increases the pH value in all the eluates (Es). Unlike the BLT, when adding 5 wt.% of PC8, the pH value of eluates decreases progressively as the L/S ratio of 10 L/kg increases. The first five eluates were within the range of minimum solubility of pH-dependent metal(oids)s (pH 8.5–10.5), but upon eluate number 6 (E6), the pH value decreased until 7.60 for E7 (eluate number 7). This decrease in pH value is due to the low reactivity of PC8 (as shown in Figure 4) and the consumption of the MgO contained in this LG-MgO (Table 5). On the other hand, when adding 10 and 15 wt.% of PC8, the pH value increased during the first four eluates (E1–E4) until a value of 10.1 for 10 wt.% of PC8 and around 10.4 for 15 wt.% of PC8. After the E4, the pH values obtained in E7 decreased until a pH of 8.46 adding 10 wt.% of PC8 and 9.39 adding 15 wt.% of PC8. Taking into account the pH values of the last fraction number (E7), with an L/S ratio of 10 L/kg, the minimum percentage needed to maintain the pH in the range of minimum solubility of pH-dependent metal(loid)s was 15 wt.% of PC8 into the CONSO to obtain a proper REMSO, as LG-MgO acts as a buffering agent in the 9–11 pH range. Below and above this pH range, the pH-dependent metal(loid)s increase their mobility, and they may be re-dissolved and released into the aqueous media.

When comparing the BLT with the PCT using PC8 as a stabilizing agent, the pH values in the batch analysis were 8.54, 9.40, and 9.90, from 5, 10, and 15 wt.% of PC8, respectively. In contrast, for the same L/S ratio, the pH values of E7 for 5, 10, and 15 wt.% of PC8 were 7.60, 8.46, and 9.39, respectively. This fact can be justified by the low reactivity of PC8, which requires longer reaction times, or more vigorous conditions (i.e., BLT conditions) to achieve the equilibrium of solubility. Therefore, although the solid-liquid (S/L) ratio for both leaching tests were 1/10, the obtained results following both procedures did not coincide. Thus, while the BLT evaluates the maximum leaching potential of the pollutants (i.e., heavy metals and metalloids), the PCT evaluates the behavior of the remediated soil over a long period of time. In this case, the use of a higher percentage of PC8 ensures a higher reservoir of stabilizing agents and optimal pH conditions over a long period of time. Again, with the addition of 15 wt.% of PC8 and although all eluates (E1–E7) showed a pH value within the optimal stabilization range, the concentration of Pb was above the threshold set for hazardous waste, very high for the first L/S ratios. This fact must be justified by the presence of lead sulfate in the polluted soil, which controls the solubility of this heavy metal. As mentioned above, the contaminated soil was in lands which included slag from lead and/or fine filtering powder. This is the main reason for the high concentration of Pb in the first eluates (E1–E4). The rest of the pH-dependent heavy metals and metalloids showed concentrations in all eluates below the threshold set established for non-hazardous wastes, with most of these below limits for inert waste.

Table 7. Results of batch leaching test after the remediations.

Heavy Metals (mg·kg ⁻¹)	MCB100M				PC8			Threshold Landfill Legislation		
	CONSO	5 wt.%	10 wt.%	15 wt.%	5 wt.%	10 wt.%	15 wt.%	Inert	Non-hazardous	Hazardous
pH	6.95	8.70	10.40	10.52	8.54	9.40	9.91			
k (mS·cm ⁻¹)	2.49	6.20	7.96	7.91	5.12	9.40	8.28			
As	3.120	<0.025	<0.025	<0.025	<0.025	<0.025	<0.025	0.5	2	25
Ba	0.142	0.100	0.040	0.198	0.429	0.269	0.133	20	100	300
Bi	0.010	<0.005	<0.005	<0.005	<0.005	<0.005	<0.005	-	-	-
Cd	2.778	0.100	<0.003	<0.003	0.056	0.005	<0.003	0.04	1	5
Co	<0.030	<0.010	<0.010	<0.015	<0.018	<0.018	<0.015	-	-	-
total Cr	<0.200	<0.200	<0.200	<0.200	<0.200	<0.200	<0.200	0.5	10	70
Cr ⁶⁺	<0.200	<0.200	<0.200	<0.200	<0.200	<0.200	<0.200	-	-	-
Cu	0.364	0.100	0.155	0.156	0.080	0.106	0.136	2	50	100
Hg	<0.010	<0.010	<0.010	<0.010	<0.010	<0.010	<0.010	0.01	0.2	2
Mo	<0.005	<0.005	0.013	0.010	<0.005	<0.005	0.021	0.5	10	30
Ni	0.278	0.380	<0.353	<0.353	<0.378	<0.412	<0.353	0.4	10	40
Pb	137.7	42.7	78.0	141.3	56.4	62.6	142.6	0.5	10	50
Sb	2.101	0.010	0.029	0.040	0.006	0.009	0.009	0.060	0.7	5
Sn	0.050	<0.010	<0.010	<0.010	<0.010	<0.010	<0.010	-	-	-
V	<0.050	<0.050	<0.050	<0.050	<0.050	<0.050	<0.050	-	-	-
Zn	2.370	<0.100	<0.100	0.116	<0.100	<0.100	0.241	4	50	200

Table 8. pH, k, metal(loid)s, and Cr⁶⁺ results of the percolation column tests of the REMSO with 5 wt.%, 10 wt.%, and 15 wt.% of PC8.

PC8	Fraction Number L/S	pH	k (mS·cm ⁻¹)	mg·kg ⁻¹																
				As	Ba	Bi	Cd	Co	total Cr	Cr ⁶⁺	Cu	Hg	Mn	Mo	Ni	Pb	Sb	Se	Sn	Zn
5 wt.%	E1: 0.1	9.60	29.30	<0.05	1.02	<0.05	0.110	<0.05	<1.50	<0.20	5.83	<0.10	<0.05	0.06	0.27	998.9	<0.05	12.52	<0.25	<2.50
	E2: 0.2	9.50	34.00	<0.05	1.32	<0.05	0.070	<0.05	<1.50	<0.20	1.66	<0.10	<0.05	0.05	0.24	1711.1	<0.05	16.34	<0.25	<2.50
	E3: 0.5	9.41	27.30	<0.05	<0.05	<0.05	0.050	<0.05	<1.50	<0.20	1.24	<0.10	<0.05	<0.05	0.26	36.4	<0.05	11.14	<0.25	<2.50
	E4: 1	9.21	19.34	<0.05	0.06	<0.05	0.040	<0.05	<1.50	<0.20	0.72	<0.10	<0.05	<0.05	0.30	47.9	<0.05	5.95	<0.25	<2.50
	E5: 2	9.12	10.26	0.01	0.07	<0.01	0.037	0.006	<0.30	<0.20	0.80	<0.02	<0.01	<0.01	0.30	41.9	0.03	7.19	<0.05	0.37
	E6: 5	7.63	6.70	<0.01	0.02	<0.01	0.028	0.006	<0.30	<0.20	0.35	<0.02	<0.01	<0.01	0.27	28.9	0.02	2.92	<0.05	<0.50
	E7: 10	7.60	4.93	<0.01	0.29	<0.01	0.024	0.005	<0.30	<0.20	0.16	<0.02	<0.01	<0.01	0.25	39.2	<0.01	1.55	<0.05	<0.50
10 wt.%	E1: 0.1	9.80	34.30	0.07	0.78	<0.05	0.070	<0.05	<1.50	<0.20	1.27	<0.10	<0.05	0.07	0.48	2500.2	0.07	15.87	<0.25	<2.50
	E2: 0.2	9.88	35.00	0.06	<0.05	<0.05	0.060	<0.05	<1.50	<0.20	0.95	<0.10	<0.05	0.07	0.49	71.2	0.09	16.64	<0.25	<2.50
	E3: 0.5	10.04	27.30	<0.05	<0.05	<0.05	0.030	<0.05	<1.50	<0.20	0.84	<0.10	<0.05	<0.05	0.46	42.1	<0.05	12.14	<0.25	<2.50
	E4: 1	10.10	14.00	<0.05	<0.05	<0.05	<0.025	<0.05	<1.50	<0.20	0.23	<0.10	<0.05	<0.05	0.30	47.7	<0.05	3.33	<0.25	<2.50
	E5: 2	9.81	6.91	<0.01	0.08	<0.01	<0.005	0.006	<0.30	<0.20	0.17	<0.02	<0.01	<0.01	0.26	69.2	0.03	2.40	<0.05	<0.50
	E6: 5	8.54	6.22	<0.01	0.33	<0.01	0.006	0.005	<0.30	<0.20	0.09	<0.02	<0.01	<0.01	0.23	22.5	0.02	1.31	<0.05	<0.50
	E7: 10	8.46	4.38	<0.01	0.53	<0.01	<0.005	0.005	<0.30	<0.20	0.07	<0.02	<0.01	<0.01	0.21	26.8	0.01	0.66	<0.05	<0.50
15 wt.%	E1: 0.1	10.04	41.50	0.62	0.08	<0.05	0.090	<0.05	<1.50	<0.20	1.68	<0.10	0.39	0.11	0.63	82.9	0.20	18.45	<0.25	<2.50
	E2: 0.2	10.20	38.30	0.06	<0.05	<0.05	0.070	<0.05	<1.50	<0.20	0.93	<0.10	<0.05	0.09	0.55	225.4	0.15	16.32	<0.25	<2.50
	E3: 0.5	10.14	29.90	<0.05	<0.05	<0.05	0.040	<0.05	<1.50	<0.20	0.57	<0.10	<0.05	0.05	0.49	40.1	0.14	11.39	<0.25	<2.50
	E4: 1	10.37	9.85	<0.05	<0.05	<0.05	<0.025	<0.05	<1.50	<0.20	0.26	<0.10	<0.05	<0.05	0.36	34.1	0.08	5.17	<0.25	<2.50
	E5: 2	9.90	9.90	0.01	<0.01	<0.01	<0.005	0.008	<0.30	<0.20	0.19	<0.02	<0.01	<0.01	0.33	34.3	0.07	3.65	<0.05	<0.50
	E6: 5	9.50	5.60	<0.01	0.05	<0.01	<0.005	0.006	<0.30	<0.20	0.07	<0.02	<0.01	<0.01	0.25	33.5	0.07	1.19	<0.05	<0.50
	E7: 10	9.39	3.36	<0.01	0.40	<0.01	<0.005	0.005	<0.30	<0.20	0.04	<0.02	<0.01	<0.01	0.21	33.2	0.04	0.48	<0.05	<0.50
Limits	Inert			0.5	20	-	0.04	-	0.5	-	2	0.01	-	0.5	0.4	0.5	0.06	-	-	4
	Non-hazardous			2	100	-	1	-	10	-	50	0.2	-	10	10	10	0.7	-	-	50
	Hazardous			25	300	-	5	-	70	-	100	2	-	30	40	50	5	-	-	200

4. Conclusions

A heavily contaminated soil was remediated by using different types of LG-MgO (MCB100M, MCB100, and PC8), which differ from each other by their MgO content, particle size, and reactivity. As the reactivity and the amount of MgO increases, the acid neutralization capacity (ANC) increases, as well.

Of the three LG-MgOs tested as stabilizing agents, the MCB100M showed the highest reactivity, being classified as a soft-burnt according to the CAT, and the highest ANC. However, the by-product of magnesium PC8, even having the lowest content in MgO, has a good ANC and a lower reactivity (dead-burnt), being the most economical of the three LG-MgOs tested and can be used as it is produced and without the need for milling, which are very decisive factors for its use as a stabilizing agent for contaminated soils. Consequently, PC8 and MCB100M were the selected LG-MgOs to carry out the remediation tests of the polluted soil.

For both tested LG-MgOs, the EN 12457-4 BLT showed that only 5 wt.% of a stabilizing agent was required for the concentration of heavy metals and metalloids to be below the threshold set for their classification as non-hazardous waste; most of which were lower than limits for inert waste. With these small amounts of LG-MgO added, the stabilized soil pH only reached values around 8.5, which are in the lower range of the interval pHs established as optimal for the stabilized contaminated soils. In addition, only a small reservoir of alkali is added, which does not guarantee optimal pH conditions over a long time.

Only lead showed concentrations in leachate above the threshold for hazardous waste. In this case, the lead concentration increased as a greater amount of LG-MgO was added and the pH of the medium increased. This is due to the presence of significant amounts of lead sulfate in the contaminated soil, coming from the spent lead–acid batteries, which controlled the solubility of this heavy metal, unlike the rest of pH-dependent metal(loid)s whose solubility is controlled by the formation of the corresponding metal hydroxide.

Finally, the PCT determined that the minimum percentage needed to maintain the pH in the range of minimum solubility of heavy metals and metalloids was 15 wt.% of PC8. The addition of higher percentages of PC8 ensures a higher reservoir of stabilizing agent and optimal pH conditions over a long period. Although results of the BLT and those regarding the PCT did not coincide, both leaching tests are complementary to study the behavior of contaminated soils.

Author Contributions: All the authors have made substantial contribution regarding the conception and design of the work, the acquisition, analysis, and interpretation of the data. Specifically, Conceptualization, J.M.C.; Methodology, J.G.-P.; Software, J.F. and J.G.-P.; Investigation, J.G.-P., J.F., and J.M.C.; Writing—Original Draft Preparation, J.G.-P.; Writing—Review & Editing, J.G.-P., J.F., and J.M.C.; Funding Acquisition, J.G.-P. and J.M.C. All authors have read and agreed to the published version of the manuscript.

Funding: Magnesitas Navarras, S.A. and UTE Demimesa companies funded the research and provided access to sampling sites.

Acknowledgments: The authors would like to thank the Catalan Government for the quality accreditation given to the research group DIOPMA (2017 SGR 118). The authors also would like to thank Tubkal Ingeniería, S.L. Dr. Jessica Giro-Paloma is a Serra Húnter Fellow.

Conflicts of Interest: The authors declare no conflict of interest. The sponsors had no role in the design, execution, interpretation, or writing of the study.

References

1. Alloway, B.J. *Heavy Metals in Soils. Trace Metals and Metalloids in Soils and their Bioavailability*; Springer: Dordrecht, The Netherlands, 2013; ISBN 978-94-007-4469-1.
2. Lanza, G.R.; Ye, X.; Randhir, T.; Ries, J.B. Mechanisms and effects of acid rain on environment. *J. Earth Sci. Clim. Chang.* **2014**, *5*, 1.

3. De Figueiredo, C.C.; Chagas, J.K.M.; da Silva, J.; Paz-Ferreiro, J. Short-term effects of a sewage sludge biochar amendment on total and available heavy metal content of a tropical soil. *Geoderma* **2019**, *344*, 31–39. [[CrossRef](#)]
4. Cui, M.; Lee, Y.; Choi, J.; Kim, J.; Han, Z.; Son, Y.; Khim, J. Evaluation of stabilizing materials for immobilization of toxic heavy metals in contaminated agricultural soils in China. *J. Clean. Prod.* **2018**, *193*, 748–758. [[CrossRef](#)]
5. Yao, Z.; Li, J.; Xie, H.; Yu, C. Review on remediation technologies of soil contaminated by heavy metals. *Procedia Environ. Sci.* **2012**, *16*, 722–729. [[CrossRef](#)]
6. Hou, D. *Sustainable Remediation of Contaminated Soil and Groundwater: Materials, Processes, and Assessment*; Elsevier: Amsterdam, The Netherlands, 2019; ISBN 9780128179826.
7. Bolan, N.; Kunhikrishnan, A.; Thangarajan, R.; Kumpiene, J.; Park, J.; Makino, T.; Kirkham, M.B.; Scheckel, K. Remediation of heavy metal(loid)s contaminated soils—to mobilize or to immobilize? *J. Hazard. Mater.* **2014**, *266*, 141–166. [[CrossRef](#)]
8. Lwin, C.S.; Seo, B.H.; Kim, H.U.; Owens, G.; Kim, K.R. Application of soil amendments to contaminated soils for heavy metal immobilization and improved soil quality—A critical review. *Soil Sci. Plant Nutr.* **2018**, *64*, 156–167. [[CrossRef](#)]
9. Derakhshan-Nejad, Z.; Jung, M.C.; Kim, K.H. Remediation of soils contaminated with heavy metals with an emphasis on immobilization technology. *Environ. Geochem. Health* **2018**, *40*, 927–953. [[CrossRef](#)]
10. Calvet, S.R.; Bourgeois, J.J.M. Some experiments on extraction of heavy metals present in soil. *Int. J. Environ. Anal. Chem.* **1990**, *39*, 31–45. [[CrossRef](#)]
11. Sastre, J.; Sahuquillo, A.; Vidal, M.; Rauret, G. Determination of Cd, Cu, Pb and Zn in environmental samples: Microwave-assisted total digestion versus aqua regia and nitric acid extraction. *Anal. Chim. Acta* **2002**, *462*, 59–72. [[CrossRef](#)]
12. Sastre, J.; Rauret, G.; Vidal, M. Effect of the cationic composition of sorption solution on the quantification of sorption-desorption parameters of heavy metals in soils. *Environ. Pollut.* **2006**, *140*, 322–339. [[CrossRef](#)]
13. Sastre, J.; Vidal, M.; Rauret, G.; Sauras, T. A soil sampling strategy for mapping trace element concentrations in a test area. *Sci. Total Environ.* **2001**, *264*, 141–152. [[CrossRef](#)]
14. Vidal, M.; Santos, M.J.; Abrão, T.; Rodríguez, J.; Rigol, A. Modeling competitive metal sorption in a mineral soil. *Geoderma* **2009**, *149*, 189–198. [[CrossRef](#)]
15. Shen, Z.; Pan, S.; Hou, D.; O'Connor, D.; Jin, F.; Mo, L.; Xu, D.; Zhang, Z.; Alessi, S.D. Temporal effect of MgO reactivity on the stabilization of lead contaminated soil. *Environ. Int.* **2019**, *131*, 104990. [[CrossRef](#)] [[PubMed](#)]
16. Shen, Z.; Zhang, J.; Hou, D.; Tsang, C.W.D.; Ok, Y.S.; Alessi, S.D. Synthesis of MgO-coated corncob biochar and its application in lead stabilization in a soil washing residue. *Environ. Int.* **2019**, *122*, 357–362. [[CrossRef](#)] [[PubMed](#)]
17. Shen, Z.; Jin, F.; O'Connor, D.; Hou, D. Solidification/stabilization for soil remediation: An old technology with new vitality. *Environ. Sci. Technol.* **2019**, *53*, 11615–11617. [[CrossRef](#)] [[PubMed](#)]
18. Jin, F.; Wang, F.; Al-Tabbaa, A. Three-year performance of in-situ solidified/stabilised soil using novel MgO-bearing binders. *Chemosphere* **2016**, *144*, 681–688. [[CrossRef](#)] [[PubMed](#)]
19. Lide, D.R. *CRC Handbook of Chemistry and Physics, 2003-2004*, 84th ed.; CRC Press: Boca Raton, FL, USA, 2003; Volume 53, ISBN 0849304849.
20. Carter, C.M.; Van Der Sloot, H.A.; Cooling, D. pH-dependent extraction of soil and soil amendments to understand the factors controlling element mobility. *Eur. J. Soil Sci.* **2009**, *60*, 622–637. [[CrossRef](#)]
21. González-Núñez, R.; Alba, M.D.; Orta, M.M.; Vidal, M.; Rigol, A. Remediation of metal-contaminated soils with the addition of materials-Part II: Leaching tests to evaluate the efficiency of materials in the remediation of contaminated soils. *Chemosphere* **2012**, *87*, 829–837. [[CrossRef](#)]
22. García, M.A.; Chimenos, J.M.; Fernández, A.I.; Miralles, L.; Segarra, M.; Espiell, F. Low-grade MgO used to stabilize heavy metals in highly contaminated soils. *Chemosphere* **2004**, *56*, 481–491. [[CrossRef](#)]
23. Gray, C.W.; Dunham, S.J.; Dennis, P.G.; Zhao, F.J.; McGrath, S.P. Field evaluation of in situ remediation of a heavy metal contaminated soil using lime and red-mud. *Environ. Pollut.* **2006**, *142*, 530–539. [[CrossRef](#)]
24. Islam, M.N.; Taki, G.; Nguyen, X.P.; Jo, Y.T.; Kim, J.; Park, J.H. Heavy metal stabilization in contaminated soil by treatment with calcined cockle shell. *Environ. Sci. Pollut. Res.* **2017**, *24*, 7177–7183. [[CrossRef](#)] [[PubMed](#)]
25. Del Valle-Zermeño, R.; Giro-Paloma, J.; Formosa, J.; Chimenos, J.M. Low-grade magnesium oxide by-products for environmental solutions: Characterization and geochemical performance. *J. Geochem. Explor.* **2015**, *152*, 134–144. [[CrossRef](#)]

26. Demir, F.; Laçin, O.; Dönmez, B. Leaching kinetics of calcined magnesite in citric acid solutions. *Ind. Eng. Chem. Res.* **2006**, *45*, 1307–1311. [[CrossRef](#)]
27. Strydom, C.A.; Van Der Merwe, E.M.; Aphane, M.E. The effect of calcining conditions on the rehydration of dead burnt magnesium oxide using magnesium acetate as a hydrating agent. *J. Anal. Calorim.* **2005**, *80*, 659–662. [[CrossRef](#)]
28. UNE-CEN/TS 15364 Caracterización De Residuos. Ensayos Del Comportamiento Durante La Lixiviación. Ensayo De Capacidad De Neutralización Ácida Y Basica. 2008. Available online: <https://www.une.org/encuentra-tu-norma/busca-tu-norma/norma?c=N0040926> (accessed on 6 July 2020).
29. CEN/TS 16637-3 Construction Products-Assessment of Release of Dangerous Substances-Part 3: Horizontal Up-Flow Percolation Test. 2016. Available online: <https://standards.iteh.ai/catalog/standards/cen/a8c5bddb-392c-40fa-9fd5-26cde8a5b177/cen-ts-16637-3-2016> (accessed on 6 July 2020).
30. Van Grinsven, J.J.M.; van Riemsdijk, W.H. Evaluation of batch and column techniques to measure weathering rates in soils. *Geoderma* **1992**, *52*, 41–57. [[CrossRef](#)]
31. Formosa, J.; Chimenos, J.M.; Lacasta, A.M.; Haurie, L. Thermal study of low-grade magnesium hydroxide used as fire retardant and in passive fire protection. *Thermochim. Acta* **2011**, *515*, 43–50. [[CrossRef](#)]
32. Fernández, A.I.; Chimenos, J.M.; Segarra, M.; Fernández, M.A.; Espiell, F. Procedure to obtain hydromagnesite from a MgO-containing residue. Kinetic study. *Ind. Eng. Chem. Res.* **2000**, *39*, 3653–3658. [[CrossRef](#)]
33. Li, Y.; Yang, S.; Taskinen, P.; He, J.; Chen, Y.; Tang, C.; Wang, Y.; Jokilaakso, A. Spent lead-acid battery recycling via reductive sulfur-fixing smelting and its reaction mechanism in the $\text{PbSO}_4\text{-Fe}_3\text{O}_4\text{-Na}_2\text{CO}_3\text{-C}$ system. *JOM* **2019**, *71*, 2368–2379. [[CrossRef](#)]



© 2020 by the authors. Licensee MDPI, Basel, Switzerland. This article is an open access article distributed under the terms and conditions of the Creative Commons Attribution (CC BY) license (<http://creativecommons.org/licenses/by/4.0/>).